

The relationship between the boundary layer moisture transport from the South China Sea and heavy rainfall over Taiwan

Chuan-Chi Tu¹, Yi-Leng Chen^{2,*}, Pay-Liam Lin^{1,3}, and Po-Hsiung Lin⁴

¹Department of Atmospheric Sciences, National Central University, Taoyuan City, Taiwan

²Department of Atmospheric Sciences, University of Hawai'i at Mānoa, Honolulu, Hawaii

³Earthquake-Disaster & Risk Evaluation and Management Center, Taoyuan City, Taiwan

⁴Department of Atmospheric Sciences, National Taiwan University, Taipei City, Taiwan

Article history:

Received 26 March 2019

Revised 3 June 2019

Accepted 1 July 2019

Keywords:

Marine boundary layer jet, Moisture transport, Heavy rainfall

Citation:

Tu, C.-C., Y.-L. Chen, P.-L. Lin, and P.-H. Lin, 2020: The relationship between the boundary layer moisture transport from the South China Sea and heavy rainfall over Taiwan. *Terr. Atmos. Ocean. Sci.*, 31, 159-176, doi: 10.3319/TAO.2019.07.01.01

ABSTRACT

From the time series of Climate Forecast System Reanalysis (CFSR), rain gauge data, and case studies, two widespread heavy rainfall ($> 80 \text{ mm day}^{-1}$) periods over Taiwan during the South China Sea Two Island Monsoon Experiment (SCSTIMX) (1 to 4 June and 14 to 18 June 2017) are found to be closely related to the large moisture transport within the marine boundary layer (MBL) from the northern South China Sea [integrated vapor transport (IVT) between surface and 900-hPa level $> 220 \text{ kg m}^{-1} \text{ s}^{-1}$] to the Taiwan area. With most of the moisture confined within the boundary layer, the moisture transport to the Taiwan area mainly occurs in the marine boundary layer jet (MBLJ). For both periods, the synoptic system-related low-level jet (SLLJ) coexists with the MBLJ, which is a subsynoptic feature. The MBLJ develops and intensifies when the mei-yu trough over southern China deepens and/or the western Pacific subtropical high strengthens and extends westward. With significant upstream moisture transport within the MBL (IVT $\sim 300 - 315 \text{ kg m}^{-1} \text{ s}^{-1}$), extreme torrential rain ($> 500 \text{ mm day}^{-1}$) occurs over Taiwan during 2 to 3 June of the first widespread heavy rainfall period. During the second widespread heavy rainfall period, there are two sub-periods of MBLJs and rainfall peaks ($> 300 \text{ mm day}^{-1}$) on 14 and 17 June with lower moisture transport by MBLJs (IVT $\sim 220 - 280 \text{ kg m}^{-1} \text{ s}^{-1}$) than during the first heavy rainfall period. For both periods, the moisture-laden MBLJs lifted by terrain and/or mei-yu jet/front systems produce heavy rainfall. The moisture transport within the MBL from the northern South China Sea to Taiwan provides a useful guide to predict heavy rainfall over Taiwan.

1. INTRODUCTION

During the early summer rainy season (May to June) over Taiwan, under the influences of jet/front systems from southern China, mesoscale convective systems (MCSs), and the warm, moist prefrontal southwesterly monsoon flow, heavy rainfall frequently occurs (Kuo and Chen 1990; Chen 1992; Li et al. 1997; Yeh and Chen 1998, 2002; Ding and Chan 2005; Jou et al. 2011; Xu et al. 2012; Tu et al. 2014, 2017; Wang et al. 2017; Chen et al. 2018). From statistical analysis, Chen and Yu (1988) and Chen et al. (2005) found that the 850 - 700-hPa low-level jet (LLJ) associated with the mei-yu front, classified as a synoptic system-related low-

level jet (SLLJ) (Du et al. 2014), is closely related to the heavy rainfall ($> 100 \text{ mm day}^{-1}$) that occurred over northern Taiwan. When a SLLJ ($> 15 \text{ m s}^{-1}$) prevailed at the 700-hPa level, there was a 91% likelihood that heavy rainfall was in progress or would begin in the next day. The frequency of 700-hPa SLLJ reached a maximum 12 hrs before and 850-hPa SLLJ right at the start of extremely heavy rainfall as the SLLJ moved towards northern Taiwan from southern China (Chen and Yu 1988). Chen et al. (2005) suggested that for a heavy rainfall event ($> 100 \text{ mm day}^{-1}$), the SLLJ at 850 hPa frequently brought in warm, moist air from the South China Sea (SCS) to the Taiwan area 12 hrs prior to the occurrence of heavy rainfall. The SLLJ frequently occurs in the warm sector of the frontal system as the frontal cyclone

* Corresponding author
E-mail: yileng@hawaii.edu

initiated in the leeside of the Tibetan Plateau or Yun-Guei Plateau deepens and migrates eastward (Chen 1977, 1978; Chen et al. 1994, 1997; Chen and Chen 1995). Chen et al. (1994, 1997) diagnosed the dynamics of SLLJ through a detailed case study. They found that the SLLJ is associated with the secondary circulation of the moist baroclinic jet/front system.

Chen et al. (2007) studied the 10-year (1997 - 2006) extremely heavy rainfall event over southern Taiwan during the early summer rainy season. They identified five torrential rain ($> 350 \text{ mm day}^{-1}$) events over southwestern Taiwan during the period. These events are characterized by large ($> 220 \text{ g kg}^{-1} \text{ m s}^{-1}$) upstream low-level moisture fluxes averaged among 1000-, 925-, and 850-hPa levels, the presence of the 850-hPa high θ_e axis, and 700-hPa upward motion over southwestern Taiwan. Chen et al. (2018) found that for the widespread heavy rainfall events over Taiwan during 10 to 12 June 2012, the maximum low-level horizontal moisture fluxes ($> 330 \text{ g kg}^{-1} \text{ m s}^{-1}$) associated with the southwesterly monsoon flow occur in the planetary boundary layer with a maximum at the 950-hPa level, transporting moisture from the northern South China Sea to the Taiwan area. The strong low-level winds in the boundary layer are called the Marine Boundary Layer Jets (MBLJ) (Tu et al. 2019). For this case, in addition to the localized heavy rainfall during the passage of a jet/front system, heavy rainfall occurs on the windward slopes of the Snow Mountains ($> 1000 \text{ mm}$) and Central Mountain Range (CMR) ($> 1500 \text{ mm}$) as the strong warm, moist, low-level winds impinge on the mountains.

Tu et al. (2019) used a five-year (2008 - 2012) reanalysis composite to study the characteristics of MBLJs over the northern South China Sea during the later period of early summer rainy season over Taiwan (June). The MBLJs are mainly caused by the subsynoptic-scale pressure gradients due to a deeper mei-yu trough over southern China and/or a stronger-than-normal western Pacific subtropical high. At the jet core, the vertical wind profile resembles an Ekman spiral with a wind speed maximum near the top of the marine boundary layer ($\sim 925 \text{ hPa}$). When both MBLJ and SLLJ are present, from the moisture budget analysis for frontal systems without considering terrain effects, the horizontal moisture transport from the South China Sea to Taiwan is associated with MBLJ. The rainfall production is mainly related to secondary circulation associated with the jet/front system in the frontal zone and localized lifting related to orographic effects (Tu et al. 2019).

Chen et al. (2007) and Tu et al. (2019) studied the low-level moisture transport using composite analyses. The MBLJ is a transient feature and the low-level moisture transport associated with the MBLJ during June 2008 to 2012 is more significant as compared to the June monthly mean southwesterly monsoon flow (Tu et al. 2019). Not every frontal system affecting the Taiwan area is accompanied by a MBLJ over the northern South China Sea. In this study, we will investi-

gate: (1) the physical mechanisms for the development and evolution of the MBLJs during the South China Sea Two-Island Monsoon Experiment (SCSTIMX-2017) (Chen et al. 2020; Sui et al. 2020); (2) the relationship between the moisture transport by the MBLJ from the northern South China Sea to the Taiwan area and the occurrences of heavy rainfall over Taiwan based on time series analysis; (3) the roles of frontal lifting and orographic effects of MBLJs on enhanced rainfall for cases identified from time series analysis.

2. DATA AND METHODOLOGY

Previous studies classified two kinds of LLJs: (1) boundary layer jet (BLJ) occurring in the planetary boundary layer (PBL); and (2) synoptic system-related low-level jet (SLLJ) occurring between the 600- and 900-hPa levels (e.g., Chen et al. 1994; Du et al. 2014). Some studies identified LLJs based on the maximum horizontal wind speed ($> 10 \text{ m s}^{-1}$) at the 925-, 850-, or 700-hPa levels (e.g., Tao and Chen 1987). In this study, two criteria are used to identify the existence of a southwesterly MBLJ over the northern South China Sea: (1) maximum wind speed of more than 10 m s^{-1} below the 900-hPa level; and (2) the vertical shear of horizontal wind $> 3 \text{ m s}^{-1}$ (Du et al. 2014; Tu et al. 2019). Similar to Tu et al. (2019), if more than 60% of the grid points in the upstream box ($116 - 120^\circ\text{E}$, $19 - 22^\circ\text{N}$; black box in Fig. 1) satisfy the MBLJ criteria and the event persists for more than 6 h, that entire day (0000 - 2400 LT) is defined as a MBLJ day. A wide and long-duration MBLJ event affecting Taiwan satisfies the MBLJ day criteria. Du and Chen (2018, 2019) studied a heavy rainfall event over southern China associated with a double LLJ (coexistence of SLLJ and BLJ). In this study, we will further analyze the relationship between the moisture transport by the MBLJ and heavy rainfall occurrence over Taiwan during mei-yu season of 2017. We will also illustrate the different roles of SLLJ and MBLJ when both jets coexist during the early summer rainy season in Taiwan.

The National Centers for Environmental Prediction (NCEP) Climate Forecast System Reanalysis (CFRS) data (Saha et al. 2010) with $0.5^\circ \times 0.5^\circ$ grids at 6-h intervals and 37 pressure levels are used to delineate favorable conditions for the development/evolution of MBLJ and moisture transport in the MBL from the northern South China Sea to the Taiwan area. The rainfall data are from conventional surface weather stations and the Automatic Rainfall and Meteorological Telemetry System (Kerns et al. 2010) (> 300 stations have valid rainfall data). Dongsha (Fig. 1) sounding data (available from the Central Weather Bureau, Taipei, Taiwan or SCSTIMX project office) are used for the upstream LLJ conditions.

The vertically integrated horizontal water vapor transport (hereafter, integrated vapor transport; Zhu and Newell 1998; Lavers et al. 2012; Tu et al. 2019) is defined as

$$IVT = \sqrt{Q_\lambda^2 + Q_\phi^2} \quad (1a)$$

and the vertical integrals of the moisture transport components in the zonal (λ) and meridional (ϕ) directions are given as follows

$$Q_\lambda = \frac{1}{g} \int_{p_0}^{p_1} qu dp \quad (1b)$$

$$Q_\phi = \frac{1}{g} \int_{p_0}^{p_1} qv dp \quad (1c)$$

where q is the specific humidity in kg kg^{-1} , u is the zonal wind in m s^{-1} , v is the meridional wind in m s^{-1} , g is the acceleration due to gravity in m s^{-2} , and p_0 is surface pressure in Pa. In this study, we analysis the IVT within the boundary layer (between surface to the 900-hPa level).

3. RESULTS

3.1 Horizontal Moisture Fluxes from Northern SCS and Widespread Heavy Rainfall Events over Taiwan

There are large temporal variations in the strength of low-level southwesterly monsoon flow during the early summer rainy season over Taiwan in 2017. In this section, we will show the time series of rainfall over Taiwan, upstream winds and geopotential height at the 925-hPa level, and upstream moisture flux (qV) at the 925- and 700-hPa levels. We will also show that periods of moisture transport by the MBLJ toward Taiwan and heavy rainfall over the

Taiwan area are closely related.

From the time series along the NW-SE cross-section line (Fig. 1; the red line) across southern China, upstream of Taiwan to Luzon Island, it is clear that during the early summer rainy season of 2017, the southwesterly MBLJ ($> 10 \text{ m s}^{-1}$) occurs upstream of Taiwan ($\sim 118.5^\circ\text{E}$, 21.5°N) when the mei-yu trough over southern China deepens and/or the western Pacific subtropical high (WPSH) extends westward (during 1 to 4 June and 14 to 21 June; Figs. 2a and b). Figure 2 shows that MBLJ occurs with a deepened mei-yu trough during 1 to 4 June and 16 to 21 June, and with WPSH extending westward during 14 to 15 June (Figs. 2a and b). The MBLJ during these periods occurs between a mei-yu trough and WPSH. There are seven days (1 to 4 June, 14 June, and 17 to 18 June) that satisfy the criteria for southwesterly MBLJ days (Tu et al. 2019) during the 2017 early summer rainy season. Note that on 18 June, only the early part of the day was under the influence of a MBLJ.

Significant horizontal moisture fluxes at the 925-hPa level associated with southwesterly MBLJ ($qV > 220 \text{ g kg}^{-1} \text{ m s}^{-1}$) upstream of Taiwan ($\sim 117.5 - 119^\circ\text{E}$) (Fig. 2c), which occurred during 1 to 4 June and 14 to 18 June, are highly correlated with heavy rainfall occurrence over Taiwan (Figs. 3a and b). Average daily rainfall over Taiwan of $> 20 \text{ mm}$ occurred during 16 May, 1 to 4 June, and 14 to 18 June (Fig. 3a). During 1 to 4 June and 14 to 18 June, there are more than 20 stations that satisfy the criteria for heavy rainfall ($> 80 \text{ mm day}^{-1}$) (Fig. 3b). The upstream southwesterly MBLJ with moisture fluxes $> 220 \text{ g kg}^{-1} \text{ m s}^{-1}$ is closely related to widespread heavy rainfall over Taiwan. One, two, 83, and 130 station(s) recorded the extremely heavy rainfall of $> 200 \text{ mm day}^{-1}$ during 1 to 4 June, respectively. Seven,

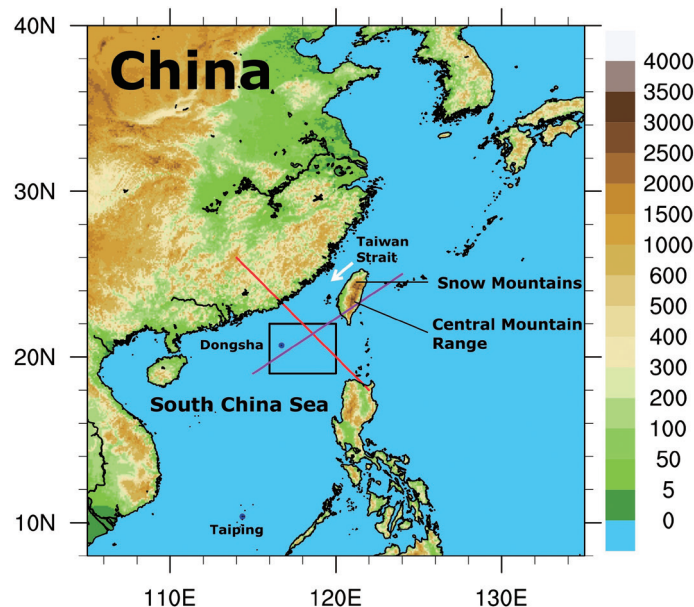


Fig. 1. Terrain height (m). The red line is the NW-SE cross-section line used for time series plot in Fig. 2. The purple line is the NE-SW cross-section line used in Fig. 9. Blue dots denote Dongsha and Taiping Islands.

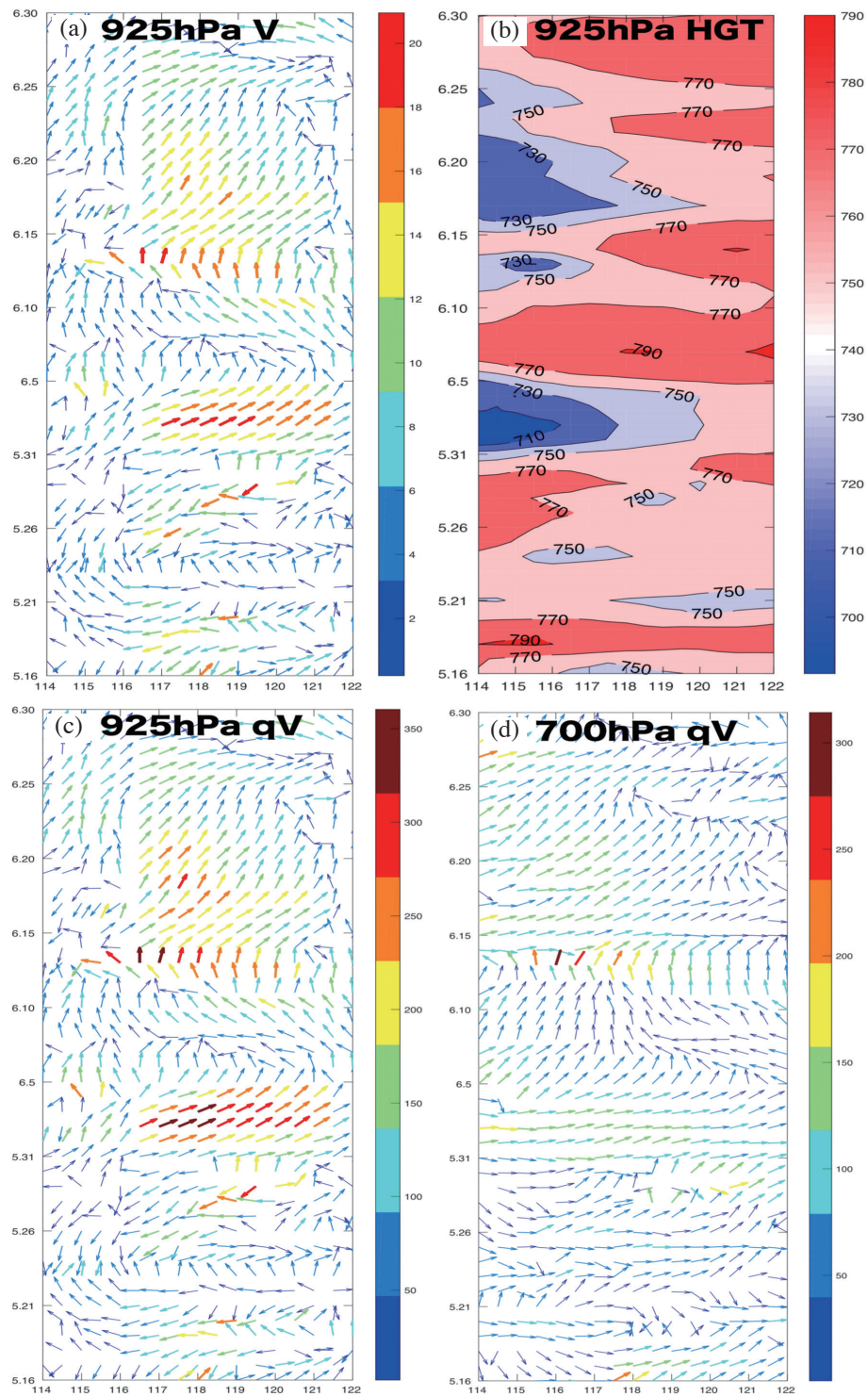


Fig. 2. The CFSR time series along the NW-SE line (red line in Fig. 1) from 0000 UTC 16 May to 0000 UTC 30 June 2017: (a) 925 hPa winds (m s^{-1}); (b) 925 hPa geopotential height (gpm); (c) 925 hPa horizontal moisture flux vector (qV) ($\text{g kg}^{-1} \text{m s}^{-1}$); and (d) 700 hPa horizontal moisture flux vector (qV) ($\text{g kg}^{-1} \text{m s}^{-1}$).

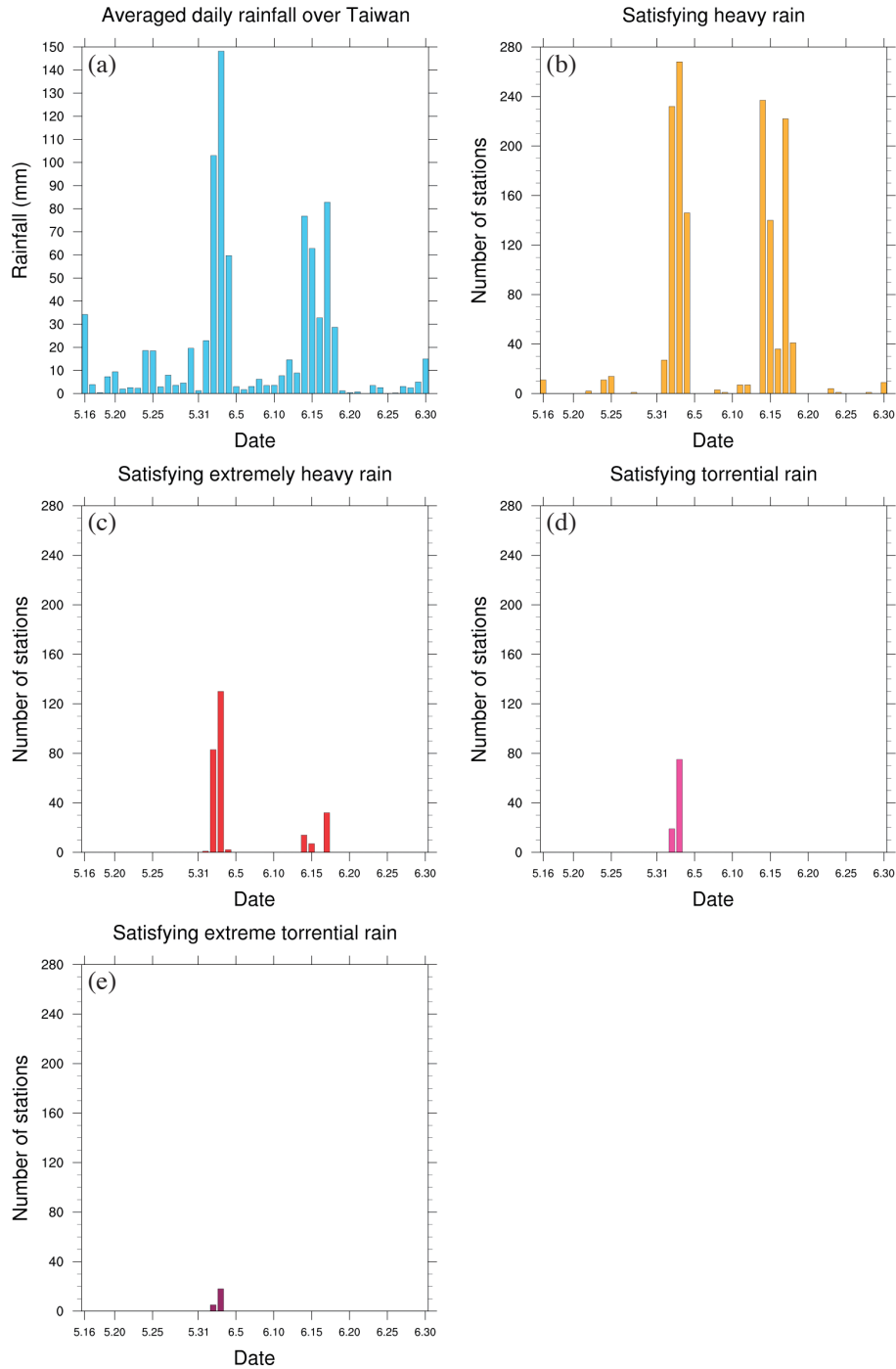


Fig. 3. Time series of (a) averaged daily rainfall over Taiwan from rain gauges (mm), (b) number of stations recording heavy rain ($> 80 \text{ mm day}^{-1}$), (c) number of stations recording extremely heavy rain ($> 200 \text{ mm day}^{-1}$), (d) number of stations recording torrential rain ($> 350 \text{ mm day}^{-1}$), and (e) number of stations recording extreme torrential rain ($> 500 \text{ mm day}^{-1}$) from 16 May to 30 June 2017 (LT).

14, and 32 stations recorded the extremely heavy rainfall of $> 200 \text{ mm day}^{-1}$ for the period 14, 15, and 17 June, respectively. Furthermore, during 2 to 3 June in the first period (1 to 4 June) the MBLJ is more intense than during the second period (14 to 18 June) with stronger winds and more significant moisture fluxes ($qV > 320 \text{ g kg}^{-1} \text{ m s}^{-1}$) within the MBL (Figs. 2a and c). As a result, the more significant moisture-laden MBLJ (Fig. 2) interacts with Taiwan's terrain and/or the surface front bringing in extreme torrential rain ($> 500 \text{ mm day}^{-1}$) over Taiwan during 2 to 3 June (Fig. 3). There are 5 and 18 stations that satisfy the criteria for extreme torrential rain ($> 500 \text{ mm day}^{-1}$) on 2 and 3 June, respectively (Fig. 3e).

During these two heavy rainfall periods, we see the co-existence of SLLJ and MBLJ upstream of Taiwan ($\sim 117.5 - 119^\circ\text{E}$) (Fig. 2). The 700-hPa SLLJ as part of secondary circulation associated with the jet/front system has much lower horizontal moisture fluxes ($qV < 160 \text{ g kg}^{-1} \text{ m s}^{-1}$) than the MBLJ (Figs. 2c and d). The high total precipitable water (TPW $> 65 \text{ mm}$) indicates the moist condition upstream of Taiwan during these two periods (not shown). Note that Tropical Storm (TS) Merbok, which occurred over the South China Sea on 12 June, and a tropical depression (TD), which occurred in the vicinity of southern China on 13 June, are not the main foci in this study.

In the following sections, we will show the evolution of large-scale weather maps and rainfall distributions over Taiwan. We will show the vertical structure of the MBLJ and the jet/front system through case studies for cases identified from time series analysis. We will also show the close relationship between the moisture transport and rainfall production through frontal lifting and orographic effects.

3.2 First Widespread Heavy Rainfall Period

During 2 to 3 June, as a surface front passes over northern and western central Taiwan, extreme torrential rain ($> 500 \text{ mm day}^{-1}$) occurs over the northern coast and the southwestern slopes of the Snow Mountains and CMR (Figs. 4b and c) with widespread heavy rainfall over Taiwan. At 0000 UTC 1 June, the mei-yu trough over southern China deepens and the WPSH extends westward into the southern South China Sea with large pressure gradients and a MBLJ ($> 16 \text{ m s}^{-1}$) presenting over the northern South China Sea (Fig. 5a). At 0000 UTC 2 June, a low in the leeside of the Yun-Guei Plateau forms within the mei-yu trough and moves over the southeastern China coast. Concurrently, the MBLJ strengthens ($> 20 \text{ m s}^{-1}$) (Fig. 5b). At 0000 UTC 3 June, the lee cyclone dissipates with weakened mei-yu trough and MBLJ (Fig. 5c). At 0000 UTC 4 June, the mei-yu trough over southeastern China continues weakening. Concurrently, the strength of the MBLJ also weakens (Fig. 5d). Note that the barrier jet (Chen and Li 1995a, b; Li and Chen 1998) off northwestern Taiwan can occur within

the boundary layer ($< 1 \text{ km}$) under an MBLJ interacting with terrain (Tu et al. 2019) as a mei-yu front approaches northern Taiwan (1 to 2 June; Figs. 5a and b). The SLLJ at the 700-hPa level has a similar tendency as the MBLJ, reaching maximum intensity on 2 June and weakening during 3 to 4 June (not shown). The mei-yu trough shows a northward tilt. The SLLJ is in the warm sector (to the south) of the mei-yu trough. In addition to the secondary circulation across the jet/front system, the winds veer with respect to height upstream of Taiwan (Figs. 2c and d), implying warm advection associated with the southwesterly monsoon flow.

The moisture transport within the MBL from the northern South China Sea to the Taiwan area corresponds well with the strength of the MBLJ with a peak on 2 June (Figs. 5 and 6). We select the upstream region along the cross-section line (red line in Fig. 1; $117.5 - 119^\circ\text{E}$) $\sim 200 \text{ km}$ away from southwestern Taiwan to analyze the upstream moisture transport within the MBL. Note that the 200 km distance is larger than the Rossby radius of deformation by orographic influence of Taiwan under the southwesterly monsoon flow ($\sim 100 \text{ km}$; Li and Chen 1998). The upstream southwesterly monsoon flow with a large IVT in the boundary layer (between surface and the 900-hPa level) ($> 230 \text{ kg m}^{-1} \text{ s}^{-1}$) (Figs. 5 and 6) brings in widespread heavy rainfall over Taiwan during 1 to 4 June (Figs. 3a - b, and 4). Note that, during 2 to 3 June, when the upstream IVT in the boundary layer exceeds $300 \text{ kg m}^{-1} \text{ s}^{-1}$ (Fig. 6), extreme torrential rain ($> 500 \text{ mm day}^{-1}$) occurs over Taiwan (Figs. 3e and 4).

From the N-S cross-section line along 118°E (Fig. 7), it is apparent that on 2 June the MBLJ exists over the northern South China Sea ($\sim 20 - 22^\circ\text{N}$) with the jet core at the 925-hPa level (Fig. 7a). The moisture transport mainly occurs in the planetary boundary layer associated with the MBLJ (Figs. 7a and c). The situation is similar on 3 June showing the existence of MBLJ, SLLJ, low-level moisture transport, and frontal upward motion (Fig. 7). From the time series of Dongsha soundings, the MBLJ with the strongest wind speed at the 925 - 950-hPa level reaches its maximum intensity on 2 June ($> 20 \text{ m s}^{-1}$) (Fig. 8a). The high moisture is mostly within the boundary layer (Fig. 8b). The sounding observations also show that the moisture transport associated with the MBLJ ($qV > 390 \text{ g kg}^{-1} \text{ m s}^{-1}$) is more significant than the SLLJ (Fig. 8c) with its maximum magnitude below the 925-hPa level.

During 2 to 4 June, the MBLJ with large moisture transport to the Taiwan area (Figs. 5 and 6) is lifted by the secondary circulation associated with the jet/front system (Fig. 7) or terrain (Fig. 9). On 2 June, orographic lifting of MBLJ is evident on the windward side with low-level convergence due to orographic blocking (Fig. 9). The second low-level convergence region east of Taiwan is contributed by the northerly flow in the west flank of lee vortex encountering the strong orographic induced southwesterly flow

southeast of Taiwan ahead of the frontal surface (Sun and Chern 1993) (Figs. 5b and 9). The SLLJ impinges on the Snow Mountains and CMR and also contributes to heavy rainfall. Localized heavy rainfall occurred along the northern coast as a combination of frontal lifting and orographic forcing as the surface front stalled along the northern coast for several hours (~0300 - 1000 LT). The mesoscale processes, including the lifting of the moisture-laden MBLJ (orographic lifting and frontal lifting), deserve further investigation in the future using high-resolution (< 3 km) mesoscale models (e.g., Weather Research and Forecasting model).

3.3 Second Widespread Heavy Rainfall Period

The second widespread heavy rainfall period over Taiwan for the 2017 early summer rainy season occurred during 14 to 18 June (Figs. 3a - b and 10) with an upstream MBLJ (Fig. 11). There are two sub-periods of MBLJ events (14 to 15 June and 16 to 18 June) during this period (Fig. 11). Prior to this heavy rainfall period over Taiwan, TS Merbok originated over the South China Sea, moved over southern China, weakened into a TD on 13 June (Fig. 11a), and then merged

with the mei-yu trough over southern China. As a result, a southerly MBLJ occurs on the southeastern flank of the TD over the northern South China Sea. Taiwan is under southerly flow without an orographic lifting component because the southerly flow is parallel to the CMR (Fig. 11a). On 14 June, the TD embedded in the mei-yu trough transforms to a frontal cyclone and moves off the southeastern China coast (Fig. 11b). The ENE-WSW oriented mei-yu trough extends from the frontal cyclone to southeastern China with the wind direction of the MBLJ changing to southwesterly. Concurrently, WPSH strengthens and extends westward resulting in the intensification of the MBLJ (Fig. 11b). On 15 June, the frontal cyclone moves eastward (not shown) with the weakened mei-yu trough and MBLJ (Fig. 11c).

On 16 June, as the mei-yu trough deepens, another MBLJ event develops (Fig. 11d). On 17 June, a mei-yu frontal cyclone moves over the southern coast of China with the intense jet core of the southwesterly MBLJ impinging on Taiwan (Fig. 11e). On 18 June, as WPSH extends westward. Concurrently, the upstream MBLJ axis shifts westward to the Taiwan Strait with a wind maximum in the southeastern flank of the frontal cyclone (Fig. 11f).

During 14 to 18 June, the large southwesterly IVT in the

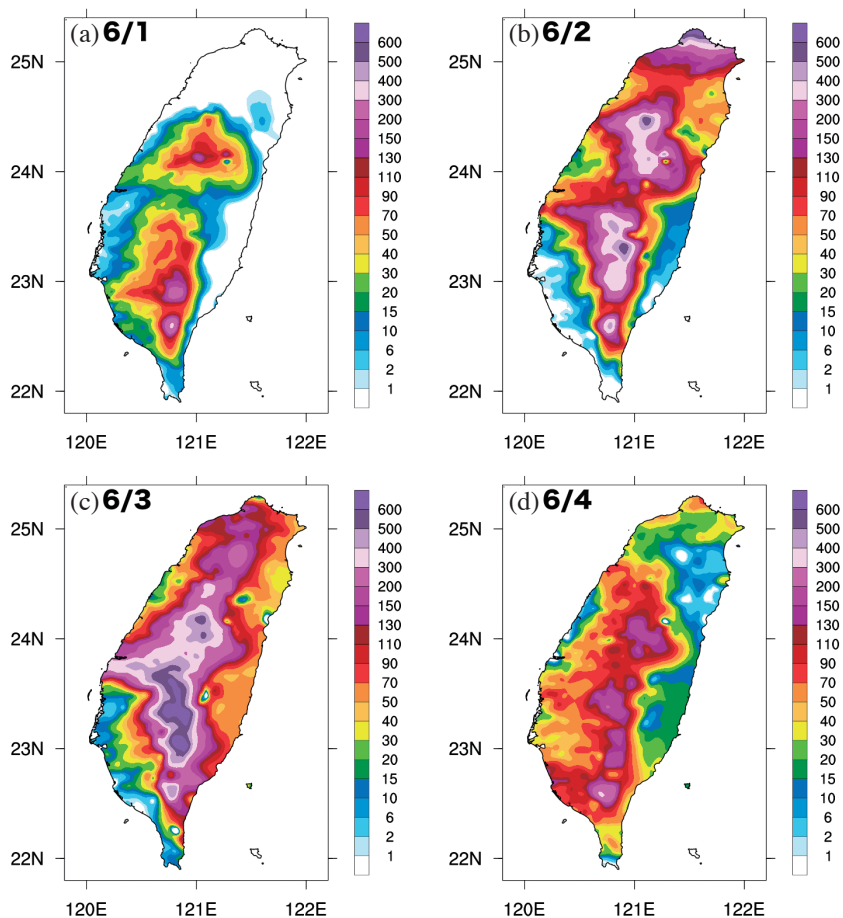


Fig. 4. Total rainfall accumulation (mm) during (a) 1 June, (b) 2 June, (c) 3 June, and (d) 4 June 2017 (LT) from rain gauge observations.

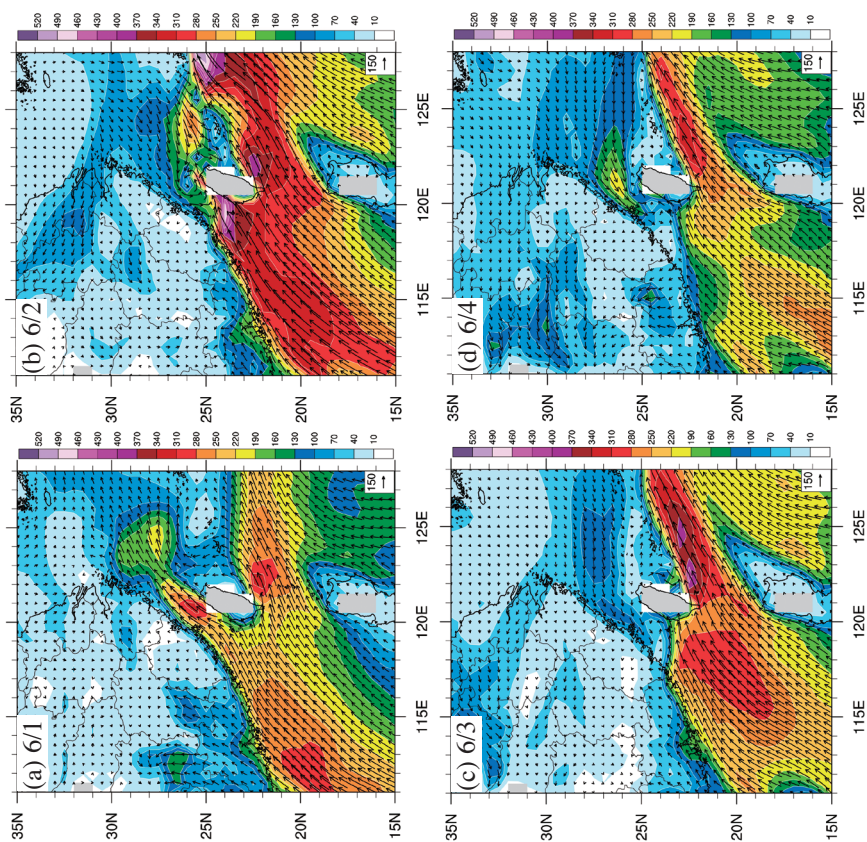


Fig. 6. The CFSR integrated vapor transport (IVT; $\text{kg m}^{-1} \text{s}^{-1}$) in the boundary layer (below 900 hPa) at (a) 0000 UTC (0800 LT) 1 June, (b) 0000 UTC (0800 LT) 2 June, (c) 0000 UTC (0800 LT) 3 June, and (d) 0000 UTC (0800 LT) 4 June 2017.

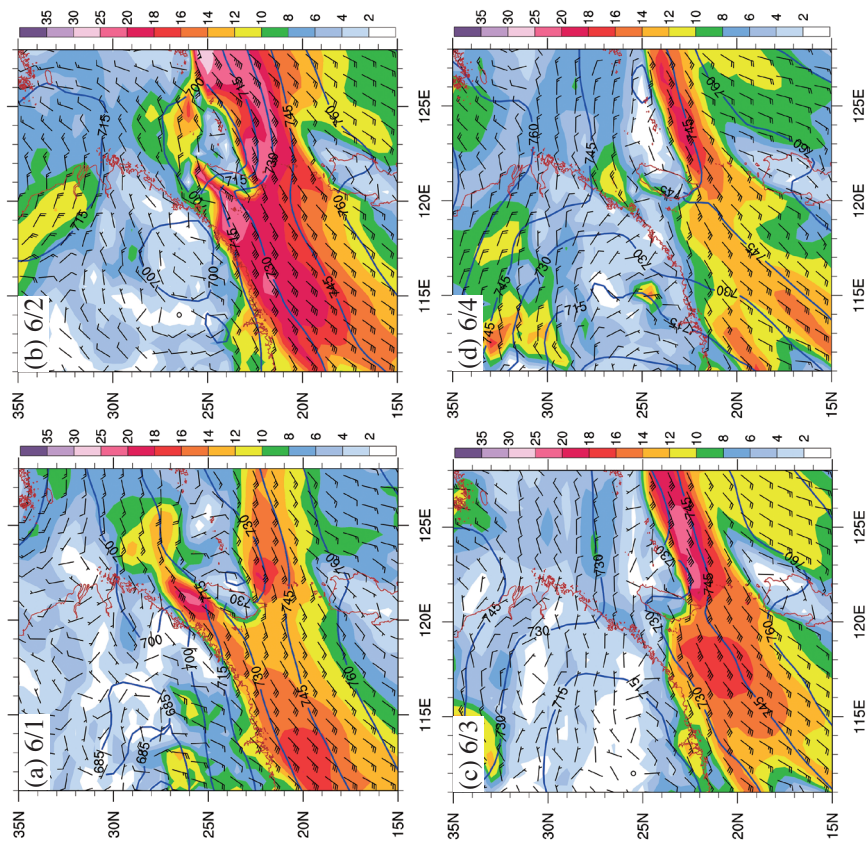


Fig. 5. The CFSR 925 hPa geopotential height (gpm, contoured) and winds (m s^{-1}) (a full barb represents 5 m s^{-1}) at (a) 0000 UTC (0800 LT) 1 June, (b) 0000 UTC (0800 LT) 2 June, (c) 0000 UTC (0800 LT) 3 June, and (d) 0000 UTC (0800 LT) 4 June 2017.

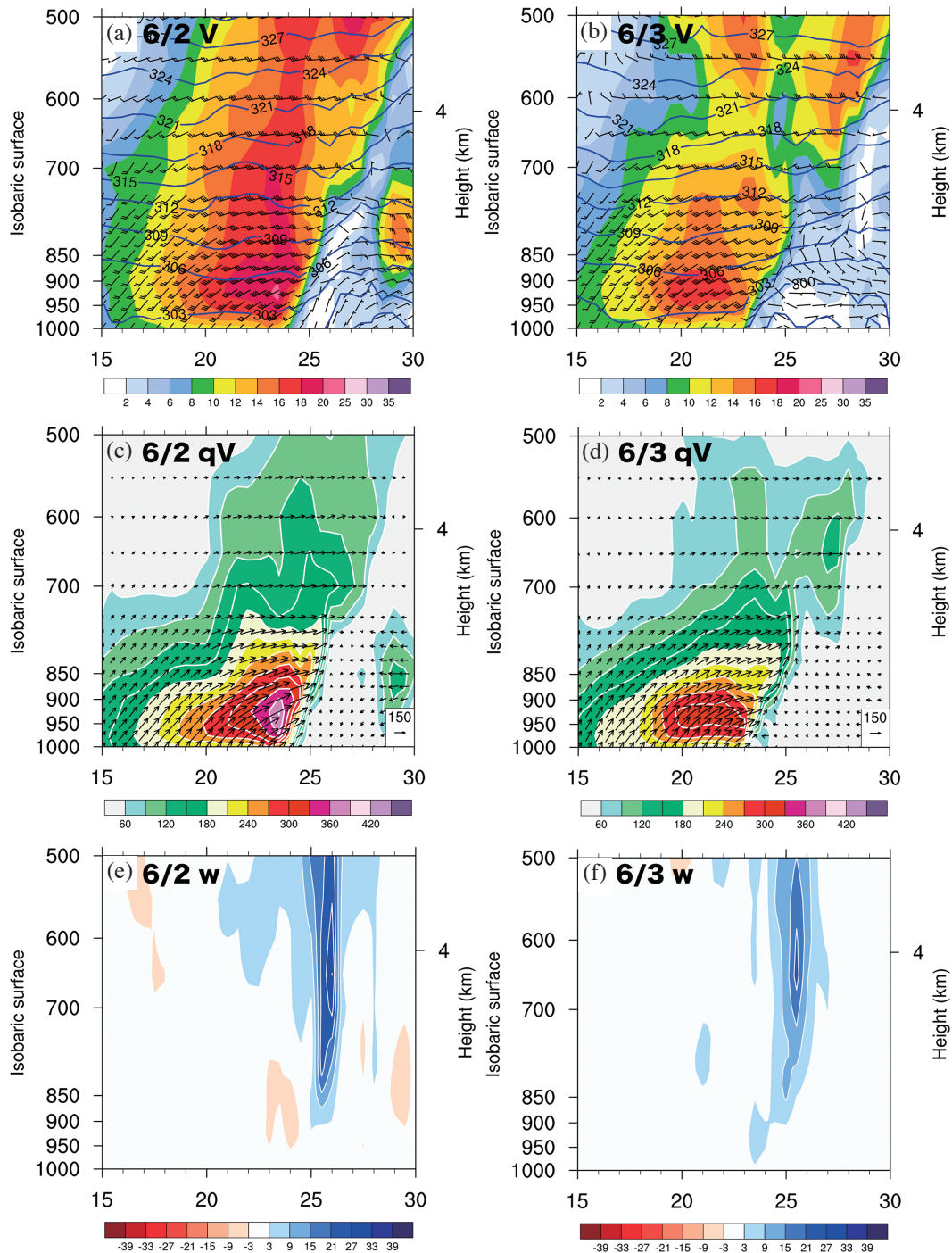


Fig. 7. The vertical cross-section of winds (m s^{-1}) (a full barb represents 5 m s^{-1}) and potential temperature (K, contoured) along 118°E at (a) 0000 UTC (0800 LT) 2 June and (b) 0000 UTC (0800 LT) 3 June 2017. (c) and (d) same as (a) and (b) but for horizontal moisture flux vector (qV) ($\text{g kg}^{-1} \text{m s}^{-1}$). (e) and (f) same as (a) and (b) but for vertical velocity (cm s^{-1}).

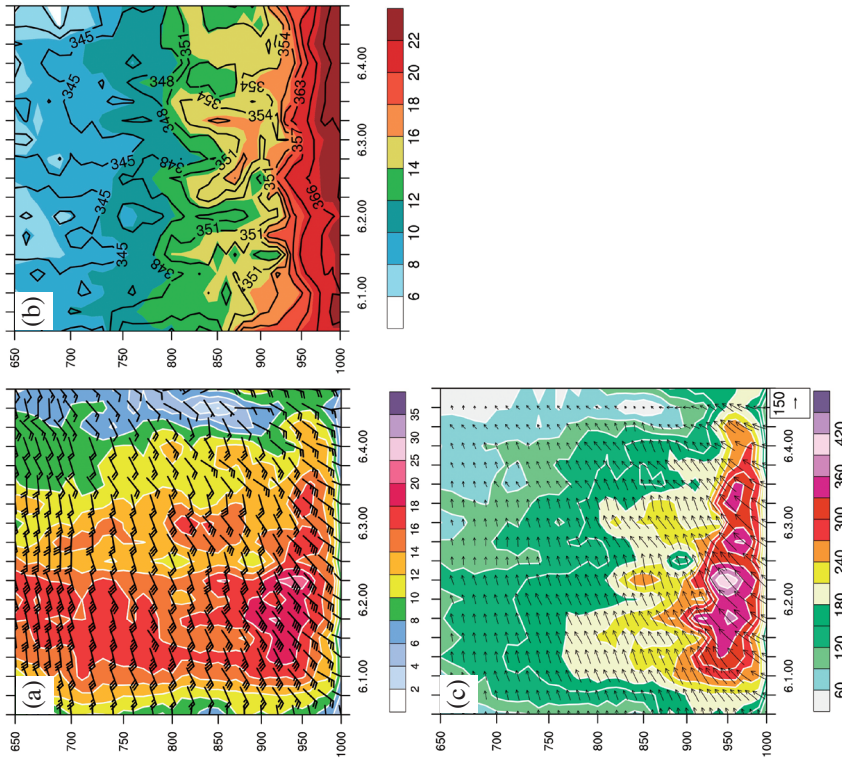


Fig. 8. (a) The time series of wind speed (m s^{-1}) (shaded) and winds (m s^{-1}) (a full barb represents 5 m s^{-1}) from Dongsha (Fig. 1) soundings during 1200 UTC (2000 LT) 31 May to 1800 UTC 4 June (0200 LT 5 June) 2017. (b) Same as (a), but for water vapor mixing ratio (g kg^{-1} , shaded) and equivalent potential temperature (K, contoured). (c) Same as (a) but for horizontal moisture flux vector (qV) ($\text{g kg}^{-1} \text{ m s}^{-1}$). (Data source: CWB and SCSTIMX project office.)

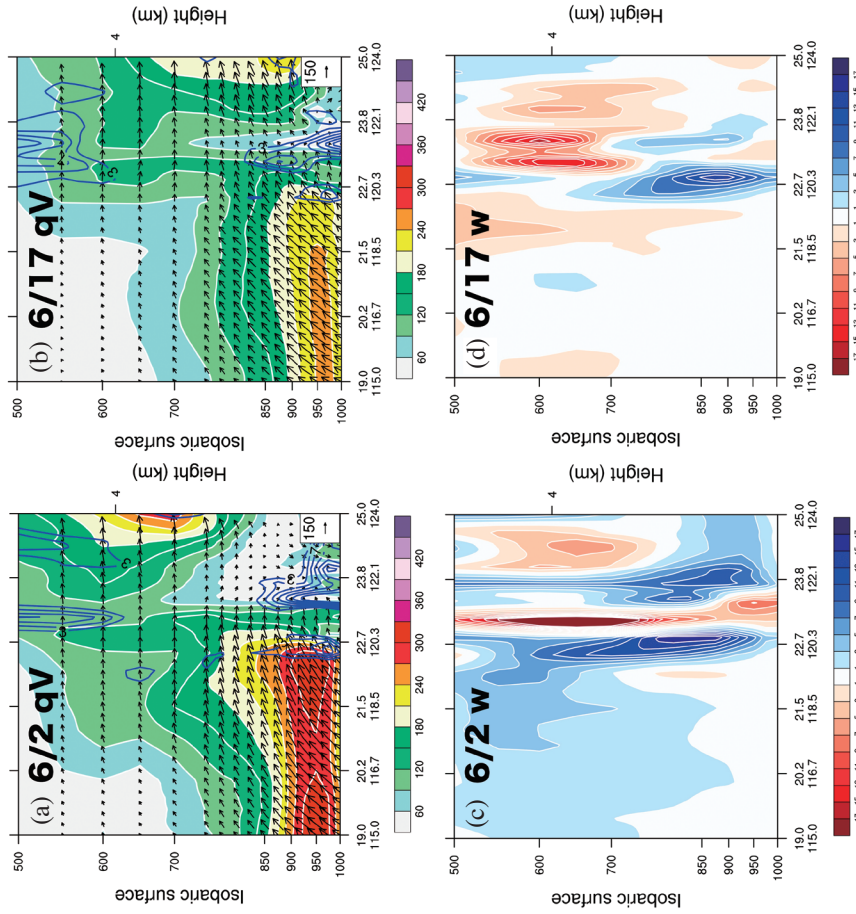


Fig. 9. The vertical cross-section of horizontal moisture flux vector (qV) ($\text{g kg}^{-1} \text{ m s}^{-1}$) and convergence (blue contours; $> 3 \times 10^{-5} \text{ s}^{-1}$, contoured every $2 \times 10^{-5} \text{ s}^{-1}$) along MBLJ direction (purple line in Fig. 1) at (a) 0000 UTC (0800 LT) 2 June and (b) 0000 UTC (0800 LT) 17 June 2017. (c) and (d) same as (a) and (b) but for vertical velocity (cm s^{-1}).

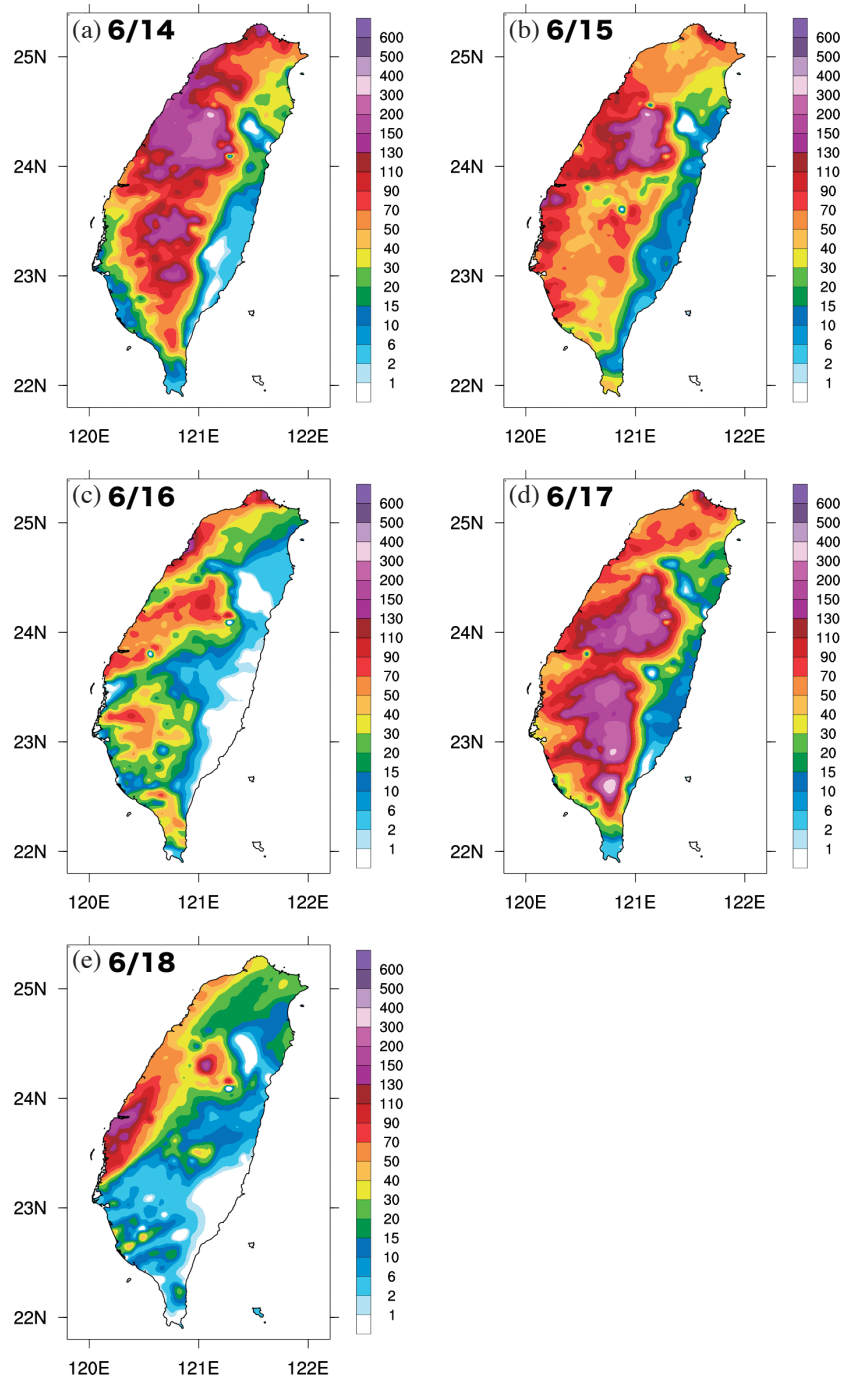


Fig. 10. Total rainfall accumulation (mm) during (a) 14 June, (b) 15 June, (c) 16 June, (d) 17 June, and (e) 18 June 2017 (LT) from rain gauge observations.

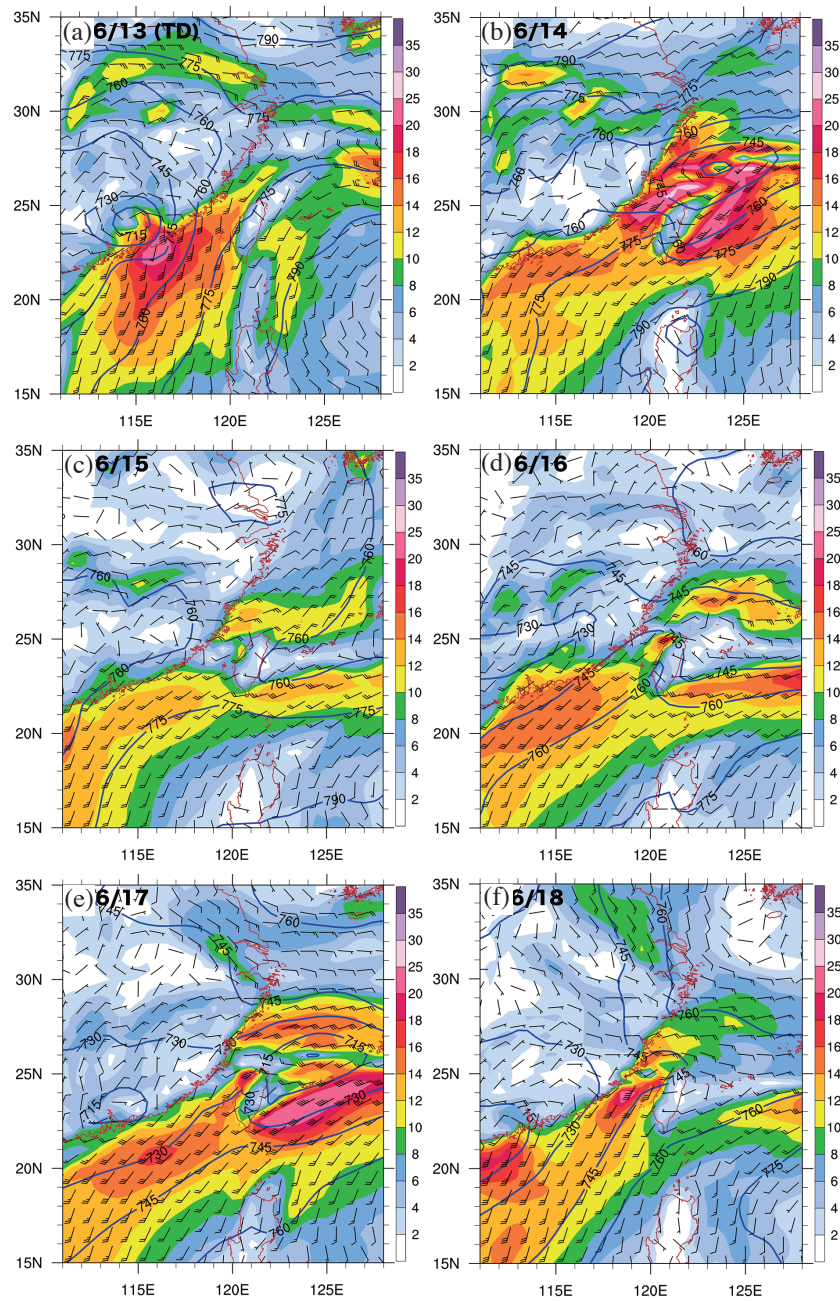


Fig. 11. The CFSR 925 hPa geopotential height (gpm, contoured) and winds (m s^{-1}) (a full barb represents 5 m s^{-1}) at (a) 0000 UTC (0800 LT) 13 June, (b) 0000 UTC (0800 LT) 14 June, (c) 0000 UTC (0800 LT) 15 June, (d) 0000 UTC (0800 LT) 16 June, (e) 0000 UTC (0800 LT) 17 June, and (f) 0000 UTC (0800 LT) 18 June 2017.

boundary layer ($> 220 \text{ kg m}^{-1} \text{ s}^{-1}$) upstream (Fig. 12) corresponds well with the widespread heavy rainfall over Taiwan (Figs. 3 and 10). The moisture transport in the MBL from the northern South China Sea to the Taiwan area (Fig. 12) corresponds well with the strength of the MBLJ (Fig. 11), showing two sub-periods (14 to 15 June and 16 to 18 June). The time series of stations satisfying extremely heavy rain ($> 200 \text{ mm day}^{-1}$) shows two separate peaks during the two sub-periods (14 stations on 14 June, and 32 stations on 17 June, respectively) (Fig. 3c) with large southwesterly IVT ($> 220 \text{ kg m}^{-1} \text{ s}^{-1}$) that extends from the northern South China Sea to Taiwan and impinges on the Taiwan terrain (Fig. 12). For the second period (14 to 18 June), there are two sub-periods (14 to 15 June, 16 to 17 June) with rainfall peaks on 14 and 17 June (Fig. 3) corresponding to two peaks in IVT ($> 225 \text{ kg m}^{-1} \text{ s}^{-1}$ on 14 June and $> 255 \text{ kg m}^{-1} \text{ s}^{-1}$ on 17 June) (Fig. 12). After the shift of the axis of the MBLJ to the Taiwan Strait (Fig. 11f), the rainfall over the windward side of both the Snow Mountains and the CMR diminishes (Fig. 10e).

In addition to rainfall production on the windward of both the Snow Mountains and CMR (Figs. 10a and d) due to orographic lifting (Figs. 9b and d), both sub-periods (14 to 15 June and 17 June) are influenced by subsynoptic forcing as the jet/front system arrives (Figs. 13a and b). The horizontal moisture fluxes transported by the MBLJ to the Taiwan area (Figs. 13c and d) are lifted by the secondary circulation in the frontal zone (Figs. 13e and f).

3.4 Discussion

We investigate the entire early summer rainy season of 2017 during SCSTIMX. From the time series analysis, evolution of weather patterns, and horizontal rainfall distributions, there are two periods with MBLJ over the South China Sea with widespread heavy rainfall over Taiwan. We also show that the rainfall production over the Taiwan area is closely related to the moisture transport in the MBL as the jet/front system approaches.

For both periods (1 to 4 June and 14 to 18 June), the horizontal moisture transport mainly occurs within the MBL associated with the MBLJ. The MBLJ occurs when mei-yu trough over the southern China deepens and/or WPSH extends westward with subsynoptic pressure gradients. The MBLJ intensifies when a lee cyclone, originated in the leeside of Yui-Guei Plateau over southwestern China, deepens and moves to the southern coast of China (e.g., 2 to 3 June and 16 to 17 June) or when a mei-yu frontal cyclone, transformed from a TC/TD, is embedded within the mei-yu trough (e.g., 14 June). For the second sub-period during 16 to 17 June, there is no apparent westward extension of WPSH (Figs. 2b, 11d, and e) during the development of the MBLJ. Nevertheless, the development of all the MBLJ events are all related to an increase in pressure gradients

related to the evolution of weather patterns.

For both periods, the MBLJ is accompanied by the SLLJ (Figs. 7 and 13) with subsynoptic forcing. However, before the arrival of the jet/front system over Taiwan, the MBLJ can be lifted by the Snow Mountain and CMR (Fig. 9) producing heavy rainfall on the windward side without frontal lifting. As the jet/front system arrives, the horizontal moisture transport by a MBLJ, provides the moisture sources for the development of heavy precipitation. However, the upstream moisture transport within the MBL is more significant during the first heavy rainfall period than the second heavy rainfall period with a stronger MBLJ ($> 20 \text{ m s}^{-1}$) (Figs. 8a vs. 14a) and higher equivalent potential temperature in the boundary layer (Figs. 8b vs. 14b). As a result, the maximum rainfall during the first period ($> 500 \text{ mm day}^{-1}$) is higher than the second period ($> 300 \text{ mm day}^{-1}$) (Figs. 4 vs. 10).

Du and Chen (2018, 2019) emphasize the role of double LLJs (BLJ and SLLJ) in southern China to the convective initiation (CI) near the south coast of China, located hundreds of kilometers to the south of an inland cold front. The SLLJ in the heavy rainfall case of Du and Chen (2018, 2019) shares the same characteristics as in this study with rainfall in the frontal zone. The BLJ upstream of the southern China coast in Du and Chen (2018, 2019) reaches its maximum in the early morning, which is influenced by both the boundary processes (e.g., inertial oscillation mechanism driven by the thermal contrast between land and ocean) and large-scale circulation or weather system (e.g., enhancement of the low-pressure circulation to the west of the coastal region with west-east thermal contrast). Furthermore, the BLJ upstream of the southern China coast is strongly modified by the terrain of Hainan Island. In contrast, the MBLJ is over the open ocean and in lower latitudes. Our preliminary results show that the MBLJ reaches its maximum before sunrise and is close to geostrophic flow in the late afternoon due to mixing in the lowest levels and reduction of friction velocity during daytime (Tu et al. 2019). In the future, we will perform momentum budget to diagnose the dynamics of the MBLJ and its diurnal variations based on results from high resolution models.

4. SUMMARY AND CONCLUSION

During 16 May to 30 June 2017 of the South China Sea Two-Island Monsoon Experiment (SCSTIMX-2017), there are two periods of widespread heavy rainfall over Taiwan with high total precipitable water (TPW $> 65 \text{ mm}$) (1 to 4 June and 14 to 18 June 2017). For both periods, the moisture transport from the tropics to the Taiwan area by the warm, moist southwesterly monsoon flow mainly occurred in the planetary boundary below the 850-hPa level. The large moisture transport within the MBL (marine boundary layer) upstream from the northern South China Sea [integrated vapor transport (IVT) between the surface to the 900-hPa

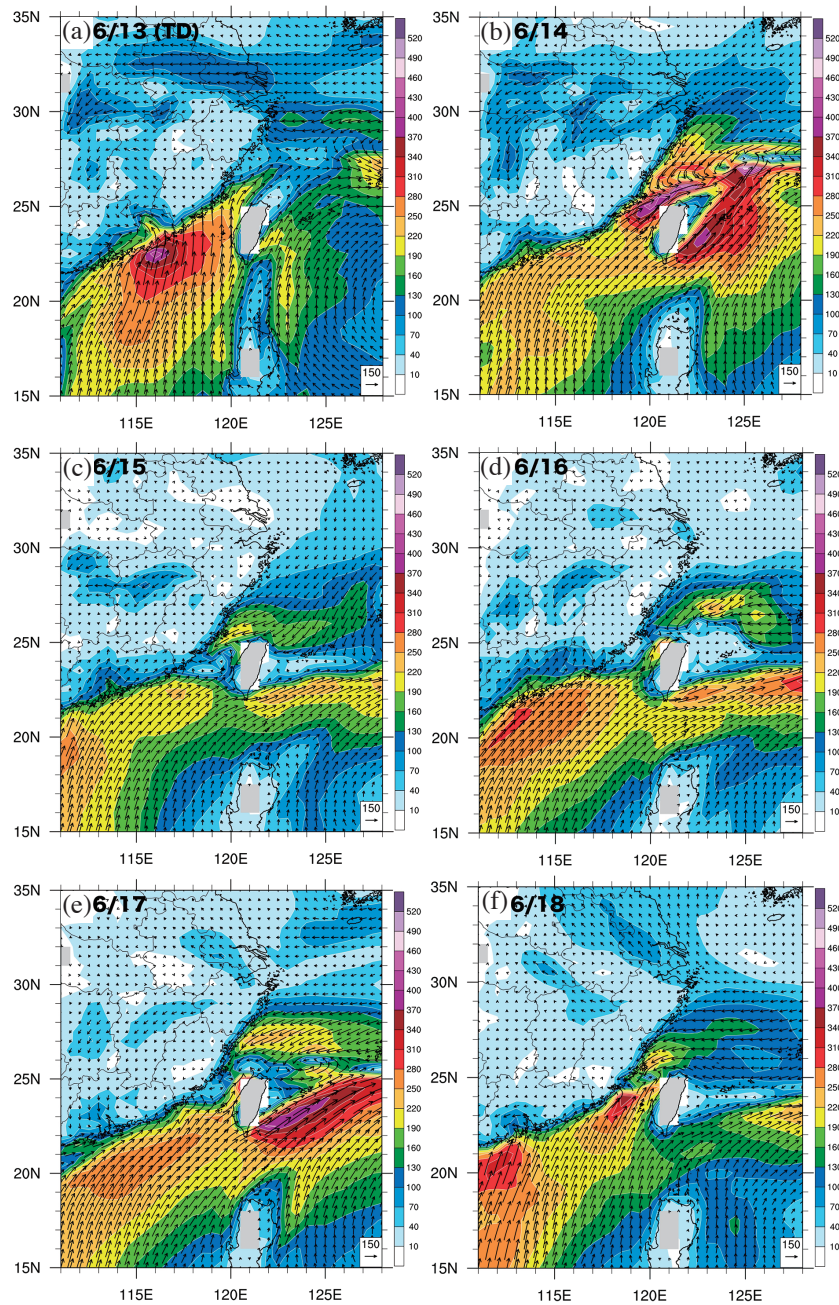


Fig. 12. The CFSR integrated vapor transport (IVT; $\text{kg m}^{-1} \text{s}^{-1}$) in the boundary layer (below 900 hPa) at (a) 0000 UTC (0800 LT) 13 June, (b) 0000 UTC (0800 LT) 14 June, (c) 0000 UTC (0800 LT) 15 June, (d) 0000 UTC (0800 LT) 16 June, (e) 0000 UTC (0800 LT) 17 June, and (f) 0000 UTC (0800 LT) 18 June 2017.

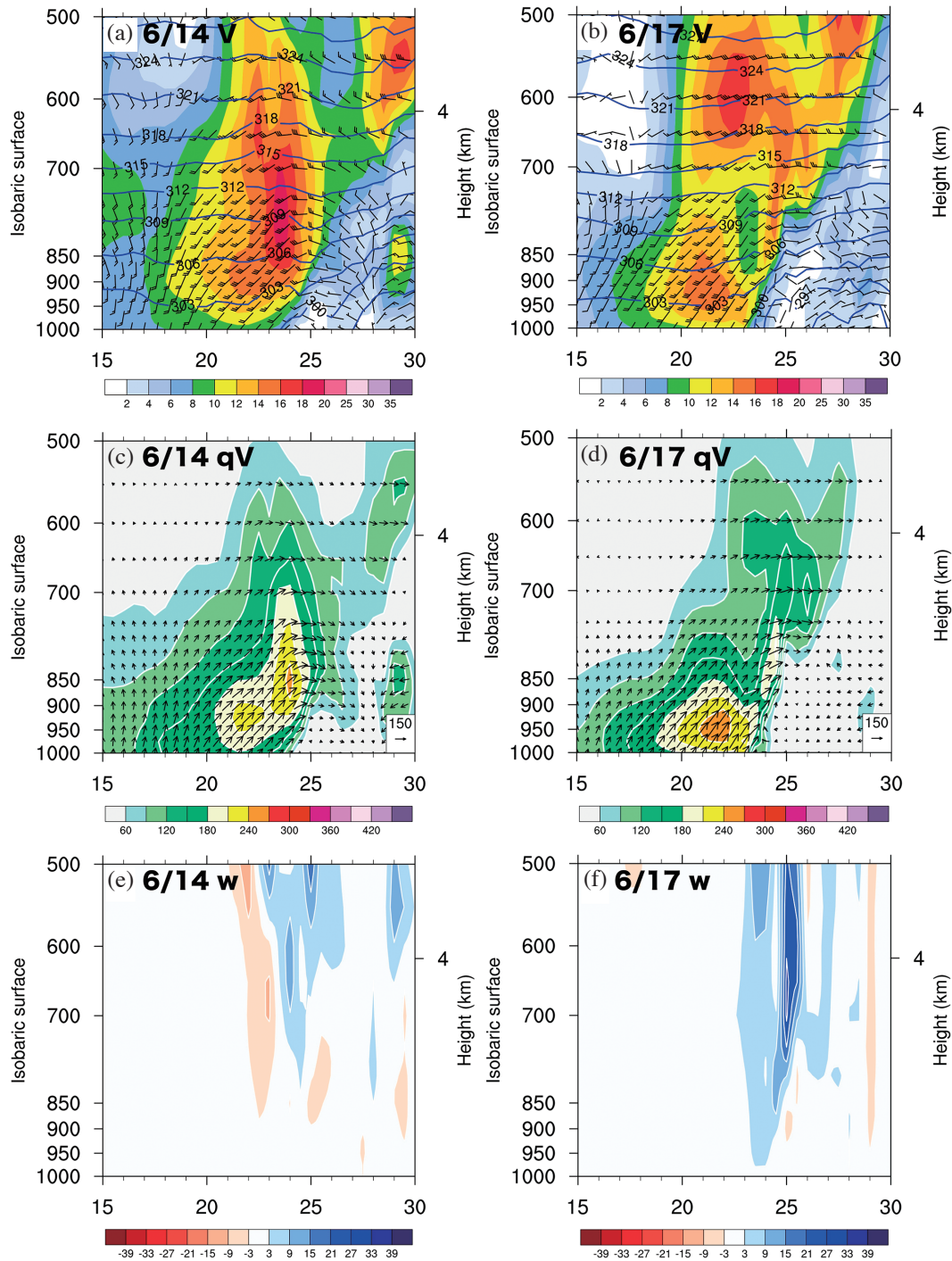


Fig. 13. The vertical cross-section of winds ($m\ s^{-1}$) (a full barb represents $5\ m\ s^{-1}$) and potential temperature (K, contoured) along $118^{\circ}E$ at (a) 0000 UTC (0800 LT) 14 June and (b) 0000 UTC (0800 LT) 17 June 2017. (c) and (d) same as (a) and (b) but for horizontal moisture flux vector (qV) ($g\ kg^{-1}\ m\ s^{-1}$). (e) and (f) same as (a) and (b) but for vertical velocity (w).

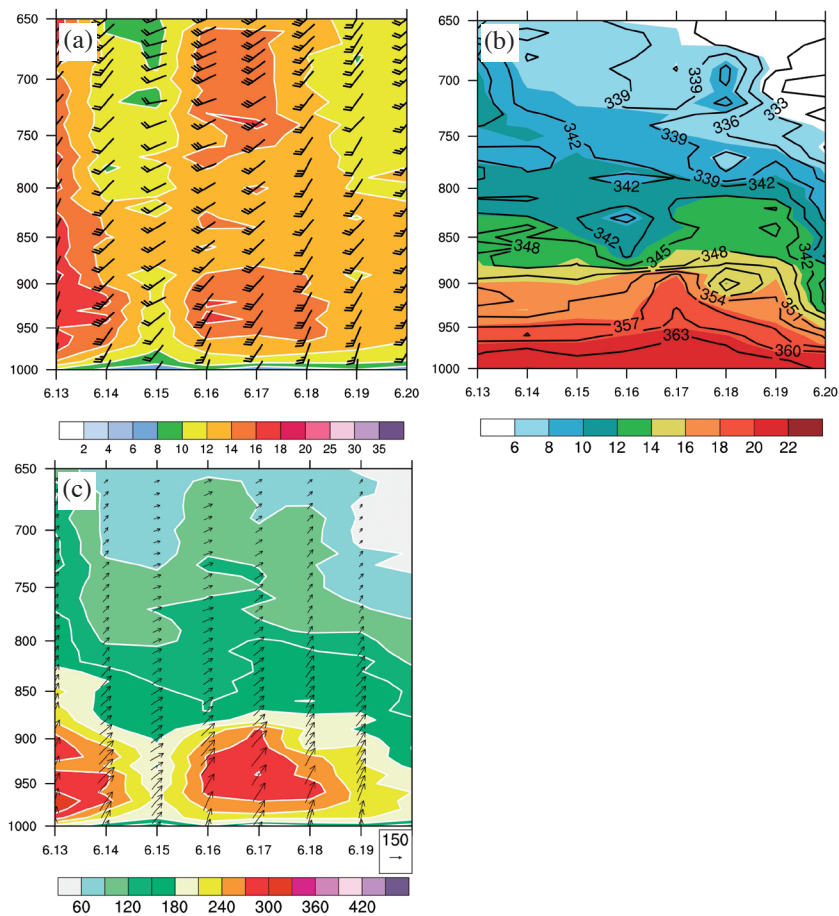


Fig. 14. (a) The time series of wind speed (m s^{-1}) (shaded) and winds (m s^{-1}) (a full barb represents 5 m s^{-1}) from Dongsha (Fig. 1) soundings during 0000 UTC (0800 LT) 13 June to 0000 UTC (0800 LT) 20 June 2017. (b) Same as (a) but for water vapor mixing ratio (g kg^{-1} , shaded) and equivalent potential temperature (K, contoured). (c) Same as (a) but for horizontal moisture flux vector (qV) ($\text{g kg}^{-1} \text{ m s}^{-1}$). (Data source: CWB and SCSTIMX project office.)

level $> 220 \text{ kg m}^{-1} \text{ s}^{-1}$] by the southwesterly MBLJ (marine boundary layer jet) brings in the widespread heavy rainfall over the Taiwan area. Over 20 stations recorded rainfall of $> 80 \text{ mm day}^{-1}$ (1 to 4 June and 14 to 18 June).

The MBLJ develops and intensifies when the mei-yu trough/cyclone over southern China deepens and/or the western Pacific subtropical high strengthens and extends westward. The MBLJ can also form when a TS/TD is embedded in the South China Sea or southern China with the presence of the western Pacific subtropical high. As the mei-yu trough/lee cyclone weakens or dissipates, the MBLJ also weakens. During the first widespread heavy rainfall period (1 to 4 June), as the mei-yu frontal cyclone moves to the southeastern coast of China on 2 June, the southwesterly MBLJ over the northern South China Sea reaches its maximum magnitude ($> 20 \text{ m s}^{-1}$). During the second widespread heavy rainfall period, there are two sub-periods (14 to 15 June and 16 to 18 June) with rainfall peaks on 14 June and 17 June. Fourteen stations on 14 June and 32 stations on 17 June recorded extremely heavy rain of $> 200 \text{ mm day}^{-1}$. On 14 June,

the intense southwesterly MBLJ is associated with a notable ENE-WSW oriented mei-yu trough, extending from a frontal cyclone northeast of Taiwan to southeastern China. Concurrently, the western Pacific subtropical high strengthens and extends westward to the South China Sea. On 17 June, as a frontal cyclone, embedded within a deepened mei-yu trough moves to the southeastern China coast, the MBLJ intensifies ($> 16 \text{ m s}^{-1}$). Furthermore, on 14 and 17 June, the intense southwesterly MBLJ with a large moisture transport within the boundary layer from the northern South China Sea to Taiwan ($\text{IVT} > 225 \text{ kg m}^{-1} \text{ s}^{-1}$ on 14 June and $> 255 \text{ kg m}^{-1} \text{ s}^{-1}$ on 17 June) impinges on the Taiwan terrain.

With significant upstream moisture transport within the MBL ($\text{IVT} \sim 300 - 315 \text{ kg m}^{-1} \text{ s}^{-1}$), extreme torrential rain ($> 500 \text{ mm day}^{-1}$) occurs over Taiwan during 2 to 3 June. During the second widespread heavy rainfall period, the moisture transport within the MBL is lower than the previous period ($\text{IVT} \sim 220 - 280 \text{ kg m}^{-1} \text{ s}^{-1}$) corresponding to extremely heavy rainfall over Taiwan ($> 300 \text{ mm day}^{-1}$). From sounding observations at Dongsha, the atmosphere is

moister ($\theta_e > 366$ K vs. 363 K, water vapor mixing ratio > 22 vs. 20 g kg⁻¹) with stronger MBLJ (> 20 m s⁻¹ vs. 16 m s⁻¹) during the first heavy rainfall period than the second period. The Dongsha sounding also shows higher moisture fluxes within the MBL during the first heavy rainfall period with a peak value ($qV > 390$ g kg⁻¹ m s⁻¹) than the second period ($qV > 300$ g kg⁻¹ m s⁻¹).

The MBLJ impinges on the Taiwan terrain and/or mei-yu jet/front systems, lasts for a few days, and brings in widespread heavy rainfall over Taiwan (1 to 4 June and 14 to 18 June 2017). The precise predictions of MBLJ and the moisture transport within the MBL are important to widespread heavy rainfall occurrences over the Taiwan area. The lifting effects of moisture-laden LLJs (especially MBLJ) by terrain and the mei-yu front deserve further research in the future using high-resolution models (e.g., Weather Research and Forecasting model).

Acknowledgements This work is jointly funded by the Ministry of Science and Technology (MOST) under Grants MOST 104-2923-M-008-003-MY5 and MOST 107-2111-M-008-038, and the Featured Areas Research Center Program within the framework of the Higher Education Sprout Project by the Ministry of Education (MOE) to the National Central University; and by the National Science Foundation under Grant AGS-1142558 to the University of Hawai‘i at Mānoa. We thank May Izumi for editing the text.

REFERENCES

- Chen, C.-S., Y.-L. Chen, P.-C. Lin, P.-L. Lin, C.-L. Liu, C.-J. Su, and W.-C. Peng, 2007: An investigation of extremely heavy rainfall events over southwestern Taiwan during the Mei-Yu season from 1997 to 2006. *Atmos. Sci.*, **35**, 287-304. (in Mandarin with English abstract)
- Chen, G. T.-J., 1977: An analysis of moisture structure and rainfall for a Mei-Yu regime in Taiwan. *Proc. Natl. Sci. Council.*, **1**, 1-21.
- Chen, G. T.-J., 1978: The structure of a subtropical Mei-yu system in Southeast Asia. *Sci. Rep. Dept. Atmos. Sci. Natl. Taiwan Univ.*, **2**, 9-23.
- Chen, G. T.-J., 1992: Mesoscale features observed in the Taiwan mei-yu season. *J. Meteorol. Soc. Jpn.*, **70**, 497-516, doi: 10.2151/jmsj1965.70.1B_497. [[Link](#)]
- Chen, G. T.-J. and C.-C. Yu, 1988: Study of low-level jet and extremely heavy rainfall over northern Taiwan in the Mei-Yu season. *Mon. Weather Rev.*, **116**, 884-891, doi: 10.1175/1520-0493(1988)116<0884:SOLLJA>2.0.CO;2. [[Link](#)]
- Chen, G. T.-J., C.-C. Wang, and D. T.-W. Lin, 2005: Characteristics of Low-Level Jets over Northern Taiwan in Mei-Yu Season and Their Relationship to Heavy Rain Events. *Mon. Weather Rev.*, **133**, 20-43, doi: 10.1175/MWR-2813.1. [[Link](#)]
- Chen, J.-M., C.-H. Tsou, R. Wu, and C.-H. Sui, 2020: Introduction to the special issue on South China Sea Two-Island Monsoon Experiment (SCSTIMX): Observation, simulation, and projection. *Terr. Atmos. Ocean. Sci.*, **31**, 97-101, doi: 10.3319/TAO.2020.03.19.01. [[Link](#)]
- Chen, X. A. and Y.-L. Chen, 1995: Development of low-level jets during TAMEX. *Mon. Weather Rev.*, **123**, 1695-1719, doi: 10.1175/1520-0493(1995)123<1695:DOLLJD>2.0.CO;2. [[Link](#)]
- Chen, Y.-L. and J. Li, 1995a: Characteristics of surface airflow and pressure patterns over the island of Taiwan during TAMEX. *Mon. Weather Rev.*, **123**, 695-716, doi: 10.1175/1520-0493(1995)123<0695:COAAP>2.0.CO;2. [[Link](#)]
- Chen, Y.-L. and J. Li, 1995b: Large-scale conditions favorable for the development of heavy rainfall during TAMEX IOP 3. *Mon. Weather Rev.*, **123**, 2978-3002, doi: 10.1175/1520-0493(1995)123<2978:LSCFFT>2.0.CO;2. [[Link](#)]
- Chen, Y.-L., X. A. Chen, and Y.-Z. Zhang, 1994: A diagnostic study of the low-level jet during TAMEX IOP 5. *Mon. Weather Rev.*, **122**, 2257-2284, doi: 10.1175/1520-0493(1994)122<2257:ADSOTL>2.0.CO;2. [[Link](#)]
- Chen, Y.-L., X. A. Chen, S. Chen, and Y.-H. Kuo, 1997: A numerical study of the low-level jet during TAMEX IOP 5. *Mon. Weather Rev.*, **125**, 2583-2604, doi: 10.1175/1520-0493(1997)125<2583:ANSOTL>2.0.CO;2. [[Link](#)]
- Chen, Y.-L., Y.-J. Chu, C.-S. Chen, C.-C. Tu, J.-H. Teng, and P.-L. Lin, 2018: Analysis and simulations of a heavy rainfall event over northern Taiwan during 11-12 June 2012. *Mon. Weather Rev.*, **146**, 2697-2715, doi: 10.1175/MWR-D-18-0001.1. [[Link](#)]
- Ding, Y. and J. C. L. Chan, 2005: The East Asian summer monsoon: An overview. *Meteorol. Atmos. Phys.*, **89**, 117-142, doi: 10.1007/s00703-005-0125-z. [[Link](#)]
- Du, Y. and G. Chen, 2018: Heavy rainfall associated with double low-level jets over southern China. Part I: Ensemble-based analysis. *Mon. Weather Rev.*, **146**, 3827-3844, doi: 10.1175/MWR-D-18-0101.1. [[Link](#)]
- Du, Y. and G. Chen, 2019: Heavy rainfall associated with double low-level jets over southern China. Part II: Convection initiation. *Mon. Weather Rev.*, **147**, 543-565, doi: 10.1175/MWR-D-18-0102.1. [[Link](#)]
- Du, Y., Q. Zhang, Y. Chen, Y. Zhao, and X. Wang, 2014: Numerical simulations of spatial distributions and diurnal variations of low-level jets in China during early summer. *J. Clim.*, **27**, 5747-5767, doi: 10.1175/JCLI-D-13-00571.1. [[Link](#)]
- Jou, B. J.-D., W.-C. Lee, and R. H. Johnson, 2011: An

- overview of SoWMEX/TiMREX. In: Chang, C.-P., Y. Ding, N.-C. Lau, R. H. Johnson, B. Wang, and T. Yasunari (Eds.), *The Global Monsoon System: Research and Forecast*, 2nd Edition, World Scientific Series on Asia-Pacific Weather and Climate, World Scientific, 303-318, doi: 10.1142/9789814343411_0018. [[Link](#)]
- Kerns, B. W. J., Y.-L. Chen, and M.-Y. Chang, 2010: The diurnal cycle of winds, rain, and clouds over Taiwan during the Mei-Yu, Summer, and Autumn rainfall regimes. *Mon. Weather Rev.*, **138**, 497-516, doi: 10.1175/2009MWR3031.1. [[Link](#)]
- Kuo, Y.-H. and G. T.-J. Chen, 1990: The Taiwan Area Mesoscale Experiment (TAMEX): An overview. *Bull. Amer. Meteorol. Soc.*, **71**, 488-503, doi: 10.1175/1520-0477(1990)071<0488:TTAMEA>2.0.CO;2. [[Link](#)]
- Lavers, D. A., G. Villarini, R. P. Allan, E. F. Wood, and A. J. Wade, 2012: The detection of atmospheric rivers in atmospheric reanalyses and their links to British winter floods and the large-scale climatic circulation. *J. Geophys. Res.*, **117**, D20106, doi: 10.1029/2012JD018027. [[Link](#)]
- Li, J. and Y.-L. Chen, 1998: Barrier jets during TAMEX. *Mon. Weather Rev.*, **126**, 959-971, doi: 10.1175/1520-0493(1998)126<0959:BJDT>2.0.CO;2. [[Link](#)]
- Li, J., Y.-L. Chen, and W.-C. Lee, 1997: Analysis of a heavy rainfall event during TAMEX. *Mon. Weather Rev.*, **125**, 1060-1082, doi: 10.1175/1520-0493(1997)125<1060:AOAHRE>2.0.CO;2. [[Link](#)]
- Saha, S., S. Moorthi, H.-L. Pan, X. Wu, J. Wang, S. Nadiga, P. Tripp, R. Kistler, J. Woollen, D. Behringer, H. Liu, D. Stokes, R. Grumbine, G. Gayno, J. Wang, Y.-T. Hou, H. Chuang, H.-M. H. Juang, J. Sela, M. Iredell, R. Treadon, D. Kleist, P. Van Delst, D. Keyser, J. Derber, M. Ek, J. Meng, H. Wei, R. Yang, S. Lord, H. van den Dool, A. Kumar, W. Wang, C. Long, M. Chelliah, Y. Xue, B. Huang, J.-K. Schemm, W. Ebisuzaki, R. Lin, P. Xie, M. Chen, S. Zhou, W. Higgins, C.-Z. Zou, Q. Liu, Y. Chen, Y. Han, L. Cucurull, R. W. Reynolds, G. Rutledge, and M. Goldberg, 2010: The NCEP Climate Forecast System Reanalysis. *Bull. Amer. Meteorol. Soc.*, **91**, 1015-1058, doi: 10.1175/2010BAMS3001.1. [[Link](#)]
- Sui, C.-H., P.-H. Lin, W.-T. Chen, S. Jan, C.-Y. Liu, Y.-J. Yang, C.-H. Liu, J.-M. Chen, M.-J. Yang, J.-S. Hong, L.-H. Hsu, and L.-S. Tseng, 2020: The South China Sea Two Islands Monsoon Experiment for studying convection and subseasonal to seasonal variability. *Terr. Atmos. Ocean. Sci.*, **31**, 103-129, doi: 10.3319/TAO.2019.11.29.02. [[Link](#)]
- Sun, W.-Y. and J.-D. Chern, 1993: Diurnal variation of lee vortices in Taiwan and the surrounding area. *J. Atmos. Sci.*, **50**, 3404-3430, doi: 10.1175/1520-0469(1993)050<3404:DVOLVI>2.0.CO;2. [[Link](#)]
- Tao, S. Y. and L. X. Chen, 1987: A review of recent research on the East Asian summer monsoon in China. In: Chang, C. P. and T. N. Krishnamurti (Eds.), *Monsoon Meteorology*, Oxford University Press, 60-92.
- Tu, C.-C., Y.-L. Chen, C.-S. Chen, P.-L. Lin, and P.-H. Lin, 2014: A comparison of two heavy rainfall events during the Terrain-influenced Monsoon Rainfall Experiment (TiMREX) 2008. *Mon. Weather Rev.*, **142**, 2436-2463, doi: 10.1175/MWR-D-13-00293.1. [[Link](#)]
- Tu, C.-C., Y.-L. Chen, S.-Y. Chen, Y.-H. Kuo, and P.-L. Lin, 2017: Impacts of including rain-evaporative cooling in the initial conditions on the prediction of a coastal heavy rainfall event during TiMREX. *Mon. Weather Rev.*, **145**, 253-277, doi: 10.1175/MWR-D-16-0224.1. [[Link](#)]
- Tu, C.-C., Y.-L. Chen, P.-L. Lin, and Y. Du, 2019: Characteristics of the marine boundary layer jet over the South China Sea during the early summer rainy season of Taiwan. *Mon. Weather Rev.*, **147**, 457-475, doi: 10.1175/MWR-D-18-0230.1. [[Link](#)]
- Wang, C.-C., F.-C. Chien, S. Paul, D.-I. Lee, and P.-Y. Chuang, 2017: An Evaluation of WRF rainfall forecasts in Taiwan during three Mei-Yu seasons from 2008 to 2010. *Weather Forecast.*, **32**, 1329-1351, doi: 10.1175/WAF-D-16-0190.1. [[Link](#)]
- Xu, W., E. J. Zipser, Y.-L. Chen, C. Liu, Y.-C. Liou, W.-C. Lee, and B. J.-D. Jou, 2012: An orography-associated extreme rainfall event during TiMREX: Initiation, storm evolution, and maintenance. *Mon. Weather Rev.*, **140**, 2555-2574, doi: 10.1175/MWR-D-11-00208.1. [[Link](#)]
- Yeh, H.-C. and Y.-L. Chen, 1998: Characteristics of rainfall distributions over Taiwan during the Taiwan Area Mesoscale Experiment (TAMEX). *J. Appl. Meteorol.*, **37**, 1457-1469, doi: 10.1175/1520-0450(1998)037<1457:CORDOT>2.0.CO;2. [[Link](#)]
- Yeh, H.-C. and Y.-L. Chen, 2002: The role of offshore convergence on coastal rainfall during TAMEX IOP 3. *Mon. Weather Rev.*, **130**, 2709-2730, doi: 10.1175/1520-0493(2002)130<2709:TROOCO>2.0.CO;2. [[Link](#)]
- Zhu, Y. and R. E. Newell, 1998: A proposed algorithm for moisture fluxes from atmospheric rivers. *Mon. Weather Rev.*, **126**, 725-735, doi: 10.1175/1520-0493(1998)126<0725:APAFMF>2.0.CO;2. [[Link](#)]